Adaptive Generator Tripping Scheme based on Deep Learning as Real Time Control Action for Transient Stability

JORGE ENRIQUE LEÓN CARPIO, ESTEFANIA ALEXANDRA TAPIA SUÁREZ,
DELIA GRACIELA COLOMÉ
Instituto de Energía Eléctrica,
Universidad Nacional de San Juan,
AV. Libertador General San Martín (OESTE) 1109,
ARGENTINA

Abstract: - Transient stability has typically received attention in the literature, focusing on its assessment and control under limited operational scenarios and contingencies. This often results in persistent transient stability issues, leaving the system vulnerable to imminent collapses. In this regard, this work aims to develop an adaptable tripping scheme based on the power system dynamics following a major disturbance to prevent grid blackouts due to transient stability loss. The proposed methodology takes advantage of data analysis tools based on deep learning and Phasor Measurement Units (PMUs) technologies. In this approach, the methodology involves generating a database of both operational scenarios and n-1 contingencies, labeling critical generators to be tripped to mitigate transient instability, and training a hybrid deep neural network RCNN (recurrent convolutional neural network) that constitutes the core of the tripping scheme. Following the application of the methodology in a controlled simulation environment, the RCNN model demonstrated strong performance, as it not only mitigated transient instability through minimal tripping of generation plants with an effectiveness of 92.4% but also showed potential for real-time application, as the control action accounts for latencies inherent in real-time operation.

Key-Words: - Power systems, transient stability, deep learning, PMU, generator tripping scheme, critical generators.

Received: April 29, 2024. Revised: November 11, 2024. Accepted: December 5, 2024. Published: January 20, 2025.

1 Introduction

Historically, the transient stability assessment in power systems has been conducted offline due to the computational time required to determine the system's dynamic response. This assessment involves step-by-step methods that solve the differential equations that represent the system's dynamics. For transient stability in particular, advancements in computer technology have enabled these methods, embedded in specialized simulation programs, to manage large power systems with numerous generators, while considering validated models of the elements that compose real power systems, [1], [2].

Although this methodology is highly useful for planning and studies focused on adjusting automatic generation tripping schemes, it cannot consider a large number of operating states and contingencies due to human limitations. Additionally, step-by-step methods are computationally demanding, and the rapid nature of the phenomenon renders real-time implementation impractical.

Conversely, direct methods aim to provide information on the transient stability status without performing simulations, optimizing the time for real-time application, [1], [3]. However, the main limitation of these methods lies in the complexity of managing detailed models of machines and other system components.

On the other hand, Phasor Measurement Unit (PMU) technology offers a comprehensive view of the electrical system's dynamics. Moreover, its high sampling frequency opens new opportunities to develop methodologies that can assess stability status and implement corrective control actions to mitigate unstable transient phenomena. As an example of the aforementioned, [4] presents, a methodology for evaluating out-of-synchronism conditions by utilizing the current, voltage, and phase angle of the three phases at both ends of two interconnected area power systems, allowing for the determination of such conditions before the synchronous generators lose synchronization.

Artificial intelligence has increasingly become integrated into various fields of study, yielding excellent results in classification tasks, and electrical engineering is no exception. Notable applications of this technology in this domain include [5], which addresses wind resource prediction essential data for optimizing real-time usage of this energy. Furthermore, [6] employs a neural network to determine the optimal unit commitment, dispatching the energy to meet systems demand while optimizing technical and economic parameters, achieving satisfactory results. A particularly relevant topic today is smart grids, where the paradigm of energy distribution is disrupted, leading to bidirectional energy flows and presenting new challenges for analysis. In this context, [7] utilizes machine learning techniques to predict the stability of these networks.

Considering the above, a new branch for power system stability analysis has emerged, utilizing AI tools. Their main advantages over traditional methods include faster processing speed, which is essential for timely preventive or emergency interventions; the capability to extend to a broader range of operational areas, including those with nonlinear behaviors; and reduced dependence on system or model parameters, as they can update the database based on historical data and system interactions, [1], [8].

In this context, various studies on transient stability problems have been based on AI algorithms. Notable examples include [9], where a deep learning model is trained to assess short-term stability and classify it into the categories of unstable due to loss of transient stability, unstable due to loss of short-term voltage stability (STVS), and stable. This is done before the system incurs instabilities and serves as the basis for applying corrective control actions in real time. Likewise, [1] constructs a model to predict transient stability margins using AI models and direct methods, incorporating concepts of extended equal area criterion. Finally, [10] employs AI algorithms to build special protection to address transient stability issues. This research was developed for a specific application in the Brazilian power system, where generation is disconnected in a specific plant considering contingencies in a single interconnection yielding excellent results.

However, despite advances in AI-based transient stability research, the application of corrective control actions to mitigate this instability phenomenon remains lacking. Therefore, the present research addresses the development of an Adaptive Generation Tripping Scheme (AGTS) that enables emergency control actions to mitigate system collapses caused by the loss of transient stability. This methodology surpasses traditional generation disconnection schemes by considering a significantly larger number of operational states and contingencies. Additionally, it offers advantages over direct algebraic methods by taking into account the system's dynamics, as it builds a database based on validated dynamic models.

This methodology uses as its core a recurrent convolutional neural network (RCNN) which, due to their rapid calculation times, enables the real-time implementation of the AGTS. Another common factor in the literature on transient stability assessment is that it does not account for STVS phenomena, which occur within the same time frame as transient stability. This oversight is often due to the static modeling of loads, which inhibits the occurrence of such phenomena. In this regard, the present study incorporates STVS by using dynamic load models, thereby aligning more closely with real-world conditions.

This work is organized into five sections detailing the AGTS development. Section 2 explores key concepts necessary for understanding the methodology and presents the technological and mathematical tools required for its development. Section 3 details the proposed methodology, while Section 4 presents the results of its application in a simulation environment. Finally, Section 5 highlights the most important conclusions of the work.

2 Technological and Mathematical Tools

This section presents the theoretical framework for power system stability and the necessary tools for the development of the proposed methodology.

2.1 Transient Stability

The stability of a power system is defined as its ability to return to an operational equilibrium state after being affected by a disturbance, starting from a specific initial condition, [11].

Specifically, transient stability is defined as the capability of a power system to maintain generator synchronism and achieve acceptable steady-state operating conditions after experiencing large disturbances, such as short circuits, the loss of major generation units, or significant load variations, [11]. The variable that best represents phenomena involving transient stability is the rotor angle of the machine. Eq. (1) describes the oscillations of this angle during disturbances.

$$\frac{2H}{\omega_0}\frac{d^2\delta}{dt^2} = \bar{T}_m - \bar{T}_e \tag{1}$$

where $\bar{T}_m$ represents the mechanical torque provided by the driving force acting on the machine's shaft, and $\bar{T}_e$ denotes the electromagnetic torque generated by the armature reaction; H represents the machine's inertia constant, ω_0 is the nominal angular velocity in rad/s, and δ is the rotor angular position relative to a synchronous reference frame.

For a system to be transiently stable during a disturbance, the rotor angle must oscillate around an equilibrium point. If the rotor angle continues to increase indefinitely, the machine is considered transiently unstable. Fig. 1 illustrates the rotor angle evolution of a synchronous machine over time. In Case 1, the oscillations are damped and stabilize at a constant value. Conversely, Cases 2 and 3 show significant amplitude increases, leading to synchronization loss. Case 2 experiences loss of synchronization during the first oscillation due to insufficient synchronizing torque, while Case 3 maintains synchronization initially but loses it after several oscillations as amplitude grows. This instability often occurs when post-fault conditions lack sufficient synchronizing torque and/or damping, despite corrective measures being implemented, [12].

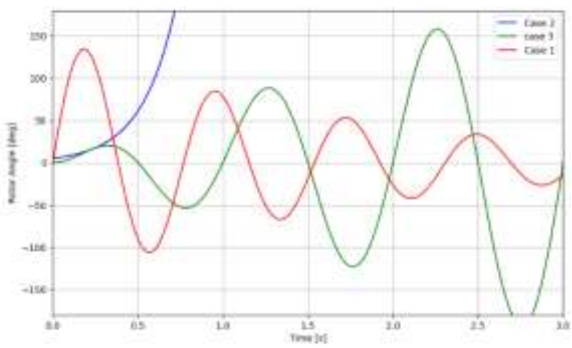

Fig. 1: Responses of the rotor angle to large disturbances

2.2 Special Protection Systems

Special Protection Systems (SPSs) execute predefined control actions post-contingency and are structured based on offline simulations where both. Static and dynamic system security are assessed, [1]. Special Protection Systems are typically characterized by [13]:

- Acting in rare contingencies that are often beyond the design range intended to withstand firm power, thereby allowing control actions not utilized under normal operating conditions, such as load and generation reductions.
- Enabling the assumption of greater operational risks, with consequences potentially exceeding the capabilities of conventional protection.
- Providing system-level protection, functioning across multiple locations, and integrating the control of various signals in a coordinated manner.

According to their control variables, SPSs can be classified into two types: event-based and response-based.

Event-based SPSs are designed to activate upon identifying a specific contingency or a combination of events, such as the loss of multiple transmission lines or generators. These event-based SPSs are faster because they do not need to wait for the system's reaction to a particular event; however, they require the evaluation of many scenarios to define their operation, [13].

Response-based SPSs are triggered based on measured electrical variables such as voltage or frequency and perform protective actions when the measured value reaches a threshold level following a contingency. Thus, they are capable of handling unplanned situations, [13].

This work aims to develop an AGTS that works as a special protection system. Unlike conventional SPSs, which consider a limited number of scenarios, the proposed scheme uses artificial intelligence algorithms that consider a vast array of operating scenarios and contingencies during its training. Additionally, similar to a response-based SPS, the proposed methodology requires measurements to assess the system's dynamics for making activation decisions and defining parameters.

2.3 Deep Learning

Artificial Intelligence (AI) encompasses the broad field of perception and knowledge extraction from data, [14]. Within AI, two principal subsets are

distinguished: Machine Learning (ML) and Deep Learning (DL). Machine Learning is a fundamental component of AI, whereas Deep Learning is considered a specialized subset of Machine Learning.

DL is characterized by employing a series of multiple layers of nonlinear processing units to automatically extract and transform features, [15]. The increase in the number of layers enhances the performance of DL methods and enables a higher level of knowledge abstraction. Although the general approach of DL is like ML, the key difference lies in the automatic feature extraction rather than manual extraction.

The DL model utilized in this work is a hybrid model composed of two DL methods: Convolutional Neural Networks (CNNs), due to their significant capacity for pattern extraction and spatial feature identification, and particularly effective in time series analysis. Conversely, Long Short-Term Memory layers (LSTMs) demonstrate strong performance in extracting temporal characteristics. Both models comprise the recurrent convolutional neural network (RCNN), which leverages the strengths of CNNs and LSTMs.

Convolutional layers aim to construct a mapping of spatial features through convolution operations applied to multidimensional data, [16]. The convolution operation is a specialized linear technique that uses a set of small matrices known as filters, which are spatially distributed across different channels. This computation involves summing the products of each filter element with the input matrix (input tensor) at each position of the tensor, yielding the corresponding value in the output matrix (output tensor), known as the feature map. On the other hand, as one of the most recognized variants of recurrent neural networks (RNNs), Long Short-Term Memory (LSTM) networks are distinguished by their ability to capture temporal features in sequential data. Furthermore, they effectively address the vanishing gradient problem, a phenomenon where gradients become so small during backpropagation that earlier layers cannot make adjustments, leading to a halt in the learning process of the neural network, [17].

The critical generator identification is achieved through the reading of power system variables via PMUs and the application of the RCNN model. The RCNN is capable of establishing a relationship between power systems variables time series and critical dynamic generation, differentiated by plants. It is important to note that the time series data encompasses a small window of the faulted state and a few samples following its clearance. The general framework of the RCNN model is presented in Fig. 2.

As illustrated in Fig. 2, the RCNN model requires specific time series data of the power system variables and transforms them into a tensor format analogous to image data. Subsequently, these data pass through the network in a cascading manner: first through convolutional layers that extract spatial features, then through LSTM layers that capture temporal features, followed by fully connected (FC) layers that integrate all extracted patterns, and finally through the classifier, that calculates the output to discriminate critical generation.

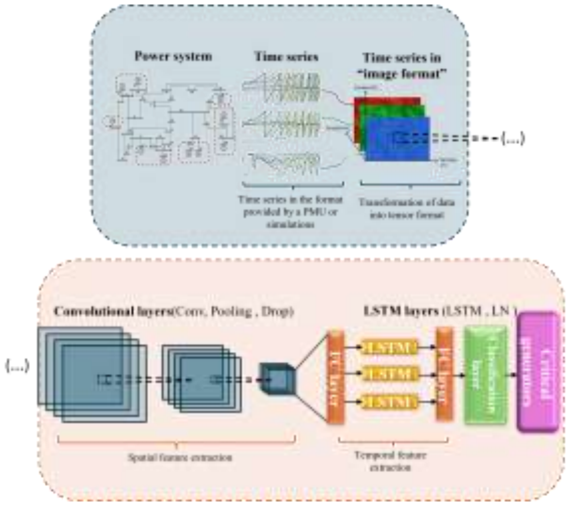

Fig. 2: General framework of the RCNN model

3 Methodology

The proposed methodology aims to identify the critical dynamic generation causing instability in cases of transient stability loss. Information on critical generation will be used to activate and adjust the AGTS parameters.

3.1 Database Generation

The creation of the database is crucial in the development of any methodology that employs artificial intelligence tools. In this regard, the data must be both sufficient and diverse to encompass a wide range of operating scenarios and system faults.

3.1.1 Operating Scenarios

The tool used to construct operating scenarios is Monte Carlo simulation, aimed at accurately representing the network's behavior. To achieve this, probabilistic models of the power system's random variables are utilized, focusing on a short-term analysis since unstable transient phenomena occur within this timeframe. Key probabilistic models needed for this short-term context, which must be developed during operational planning by the system operator, include load forecasting, unit commitment, and network topology, [18].

3.1.2 Simulationof N-1 Contingencies

In this study, N-1 contingencies are assumed to be independent and randomly generated events, including the loss of generation plants and three-phase short circuits on transmission lines. The selected contingencies are tailored to the system under study, focusing on the most likely disturbances and those that exert the greatest stress. The probability of each fault type is derived from historical data and follows a discrete probability distribution. Additionally, the fault location for short-circuit contingencies is determined using appropriate probability density functions based on historical statistics. The random generation of contingencies utilizes both uniform and Weibull distribution functions, [19].

3.1.3 Selection of Input Variables

The RCNN input data consists of a time series of power system variables. These time series must be selected to enable the accurate identification of critical generation plants within a reduced time window. In other words, the chosen variables must effectively reflect the issues that the model needs to analyze and recognize. Additionally, these variables should be measured or estimated using PMU data to ensure that the methodology can be applied in real time.

This study selects the power system variables corresponding to voltage magnitude (U), voltage angle (θ), and rotor angle (δ); all of them located in generation buses as inputs. The voltage magnitude reflects the STVS phenomena considered in this work and is measured by PMU devices. The voltage angle, according to various studies, [20], [21]. Provides information about the synchronism state of machines and is also measured by PMUs. Finally, the rotor angle directly indicates the synchronism state of generators, and currently, this variable is estimated with certain types of PMU, [22].

It is crucial to highlight that these variables (U, θ, δ) are the only inputs considered by the model. In other words, the proposed methodology is not affected by the network topology or the location of the fault. This suggests that the methodology can be applied to any network, as long as a solid database is established through simulations within that network. In line with the above, it is also important to note that if there are changes in the network topology and in the generation fleet, a new database must be created, and the model should be retrained.

3.1.4 Identification of Critical Generators

To generate the labeling of critical generators for RCNN training, it is necessary to identify the generation plants responsible for instability in each case of transient stability loss. These cases are distinguished from those unstable due to STVS, which may occur within the same time window in the generated database, [9].

In this regard, a tripping ranking is created for each case. This ranking is used to identify, through dynamic simulations, the plants whose tripping allows the system to maintain stability. The methodology for this process is described in detail below.

- **Tripping ranking:**

The first step in identifying critical generators is to create a tripping ranking. This involves tripping generation plants that have reached the theoretical stability limit one by one, based on the time it takes for each machine's rotor angle to reach the stability limit (180° or -180°), [22]. To better understand this process, two unstable cases in the IEEE New England 39-bus system are provided to illustrate how the ranking is constructed. In this case, transient instability is caused by a three-phase fault on a different transmission line in similar operating states where they are operating close to their technical limits. The response of the rotor angles of the system's machines to these events obtained through simulation in the software DigSilent Power Factory are shown in Fig. 3 and Fig. 4.

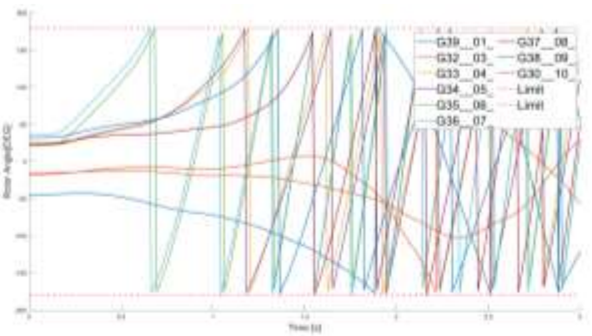

Fig. 3: Evolution of rotor angles Case 1

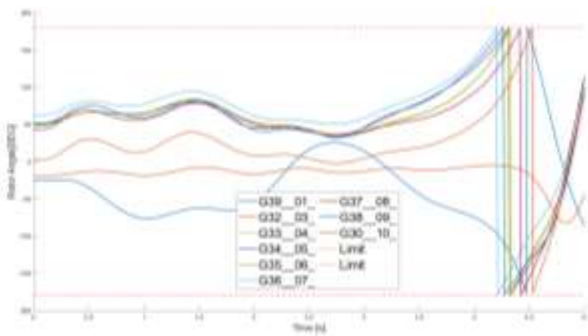

Fig. 4: Evolution of rotor angles Case 2

Fig. 3 and Fig. 4 illustrate the rotor angles of the machines. The occurrence of the faults is visible 100 ms after the simulation starts, with a successful clearing 100 ms later. According to the chosen methodology, the ranking for these cases is determined in Table 1 where the generators are presented from left to right in the order in which they lost synchronism.

In Fig. 3, it can be observed how generators G30, G33, G34, G36, G37, G38, and G39 rapidly lose synchronization following the fault, with the first two to lose synchronization being generators G36 and G35. It is important to note that 8 out of the 10 available generators in the system lose synchronization between 0.5 seconds and 2 seconds.

On the other hand, in Case 2 (Figure 4), it can be observed that although the loss of synchronization is slower, 8 out of the 10 available generators lose synchronization like in case 1, with generator G36 being the first to do so.

Table. 1 Example's disconnection ranking

Case									
Case 1	Generator	G36	G35	G34	G33	G38	G37	G39	G30
	Ranking	1	2	3	4	5	6	7	8
Case 2	Generator	G36	G38	G34	G35	G33	G37	G39	G30
	Ranking	1	2	3	4	5	6	7	8

- **Labeling of critical generators:**
After obtaining the necessary input to identify the critical generators, an algorithm was developed to perform dynamic simulations by tripping generators according to the ranking until the system remains in a stable state.

Returning to the previously mentioned cases, to illustrate the methodology, the final dynamic simulations are shown in Fig. 5 and Fig. 6. In case 1, instability has been avoided by disconnecting only the two first generators in the ranking (G36, G35) while in case 2 it only requires the tripping of the first generator in the ranking (G36). Thus, these generators will be the only ones labeled as a critical generators in each case, providing the necessary information for training the machine learning models.

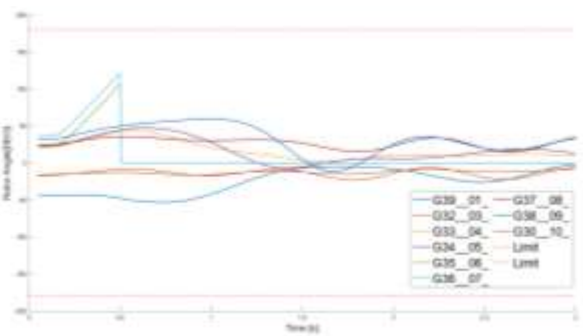

Fig. 5: Evolution of rotor angles after critical generators disconnection, G36, and G35, Case 1

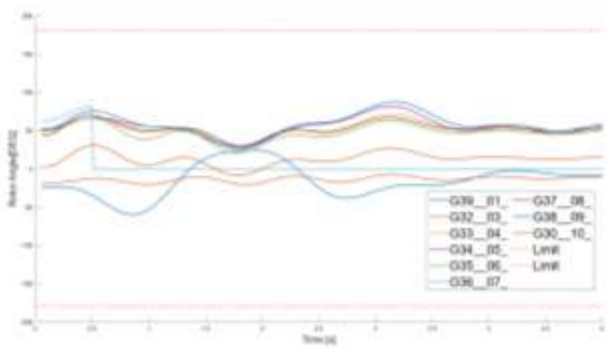

Fig. 6: Evolution of rotor angles after critical generator disconnection, G36, Case 2

3.2 RCNN Model

3.2.1 Data Preprocessing

Initially, the data must be represented in a format that the initial layers of the model, specifically the convolutional layers, can process. This format refers to a multidimensional tensor analogous to images, where the three axes correspond to the number of buses (B), number of samples (T), and number of selected variables from the power system, respectively.

The first axis represents the number of samples (T) within a time window chosen considering calculation times, switch operation times, and other latencies to enable an early avoidance of instability. The second axis represents the number of buses (B) where electrical variables are monitored. It is important to note that in this study, these buses are those with generator plants. At last, the third axis consists of the three time series variables (U, θ, δ),

which are voltage magnitude, voltage angle, and rotor angle of the machine, respectively. Therefore, the input tensor for the RCNN model has the shape (U, θ, δ) ∈ R^(15×9×3).

Finally, the dataset must be divided into a training set, a validation set, and a test set, where each element has its corresponding critical generator label. It is important to note that the labels for data from stable time series and those unstable due to short-term voltage instability will be zeros, as the model's duty is not to disconnect critical generation in these cases. The data split is performed by randomly shuffling into 70% for training, 15% for validation, and the remaining 15% for testing.

Additionally, a normalization process is necessary due to the different scales of the variables in the time series data. In this context, the z-score normalization algorithm is implemented, which ensures that each feature has a mean of 0 and a variance of 1, thereby placing the data on the same scale, [23].

3.3 Performance Metrics

Considering that the model predicts a set of classes corresponding to a set of generator plants, its performance should be evaluated using similarity sets. To assess the model's performance, the Jaccard Index is used, which estimates the similarity between two sets of integers, [24], eq. (2).

$$J(S_i, S_j) = \frac{|S_i \cap S_j|}{|S_i \cap S_j|} = \frac{|S_i \cap S_j|}{|S_i| + |S_j| - |S_i \cap S_j|} \quad (2)$$

where $J \in [0,1]$ y $J\ (si,\ sj) = 1$. In this case, a classification is considered correct when $J(\tilde{Gc}, Gc) = 1$.

The Jaccard Accuracy Index (JACC) evaluates performance across all samples, including both stable and unstable samples. When the model evaluates stable and unstable cases due to STVS, predictions of empty sets of critical machines are expected. Similarly, the Jaccard Accuracy Index for unstable samples (JACCU) calculates performance considering only unstable samples.

To conclude this section, the Jaccard Effectiveness Index (JACCUE) is used to assess whether the predicted set of machines is enough to mitigate the development of transient instability. Consequently, if the model identifies fewer or different generators than those labeled, it will not be able to mitigate the phenomenon. In this sense, this index reflects the degree of effectiveness of the task within transiently unstable samples, which is the objective of the work.

4 Results Analysis

The chosen test system for applying the proposed methodology is the IEEE New England 39-bus system. This system was selected due to its effective performance as a test system in various studies addressing similar tasks, such as the classification of short-term stability state. [9] and the evaluation of transient stability margins [1], both of which employ machine learning techniques as a core component. The system comprises 39 buses, 10 generators representing generation plants with parallel connected synchronous generators, 19 loads, and 46 transmission lines operating at a voltage level of 345 kV and a frequency of 60 Hz.

On the other hand, to accurately represent the transient stability phenomena, the standard model for RMS simulations (sixth-order subtransient model) is used in the DigSilent PowerFactory software [25] as the model for the synchronous machine generator. Similarly, to account for STVS occurring within the same time window as transient stability, a dynamic load model presented in [26] is considered.

The simulations in this section were carried out on a computer with a 64-bit Windows 10 Home operating system, and an i5-7400 CPU with 8GB of RAM.

4.1 Evaluation of Critical Generators

The first step in identifying critical generators that is, the set of generators whose tripping after a significant disturbance allows the rest to remain in synchrony is to establish a tripping ranking. This ranking facilitates the tripping of generators one by one until the system remains stable within a five-second window.

Fig. 7, presents the sets of cases, including both the unstable generators classified in the ranking and the critical generators identified by applying the proposed methodology where the tripping of this set mitigates transient stability issues.

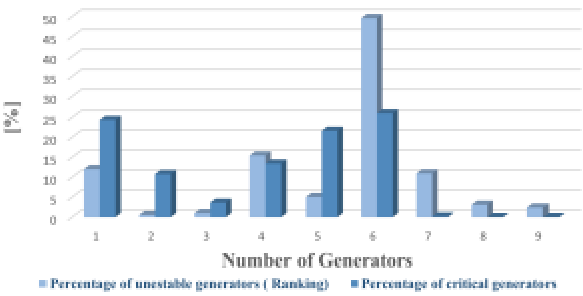

Fig. 7: Number of Unstable Generators vs. Number of Critical Generators

As shown in Fig. 7 the case of six plants to disconnect, it is observed that the set of unstable machines is 50%, while only 22% of these cases require the tripping of that many machines. Similarly, it can be noted that approximately 5% of the cases are groups of eight and nine unstable plants, while in reality there is no need to trip such groups. A similar situation occurs when only one generator needs to be tripped, where the ranking shows around 12% of cases in this category, while after applying the proposed method, this percentage increases to 24% of the cases.

This concludes that, although a large group of plants may lose stability after a significant disturbance, total tripping is not necessary. Therefore, through this methodology, a substantially smaller number of tripped generator plants can avoid instability.

4.2 Design and Model Training

4.2.1 Model Design

Training DL models begins with configuring their design, it means, involves selecting the hyperparameters that the RCNN model will use to find the most suitable parameters for correctly mapping inputs to classify labels or objectives. Hyperparameters are values defined before starting the learning process, and they can be adjusted to directly influence the model's performance. On the other hand, parameters related to the model’s weights and biases are computed during training using an optimization algorithm, [27].

The goal of model training is to find the parameters that minimize the difference between the model's predictions and the true classification of labels. In this regard, the objective function to be minimized and the optimization algorithm for learning parameters are crucial for obtaining good results.

The objective function estimates the similarity between the model’s predictions and the true classification states, while the optimization algorithm is responsible for updating the parameters iteratively to minimize this objective function. In this context, the chosen objective function and optimization algorithm are weighted cross-entropy and Adam, respectively, due to their excellent performance in classification tasks, [28], [29].

Based on the architecture of deep learning models for short-term stability studies, specifically the one proposed in [9], and to achieve high performance in the classification process, the architecture shown in Fig. 8 was designed. The hyperparameters adjusted in this architecture include the number of convolutional layers, the size and number of filters, the max pooling operations, the dropout probability, the number of LSTM layers, the number of fully connected layers, the activation functions, and the normalization layers.

In Fig. 8, the hierarchical CNN module (blocks in blue) consists of three convolutional layers, each with a different number of filters (64, 32, and 4) and a uniform size of 3×3. Additionally, the ReLU activation function is used in these layers. To prevent overfitting, max pooling with a size of 2×2, batch normalization, and dropout with a rate of 0.1 is incorporated.

Next, the flattening process is applied, which converts the spatial feature tensor into an onedimensional flat array, allowing this information to pass through 32 fully connected layers, also using ReLU as the activation function. The output of this process is directed to the hierarchical LSTM module, which adjusts 128 neurons to function as the memory unit, using tanh as the activation function. Layer normalization is also included to stabilize the training of this recurrent architecture. The extracted temporal features are then passed through 64 FC layers with ReLU activation and subsequently to the multi-layer classifier, which consists of 9 neurons responsible for performing binary classification of the system's generators. Finally, a sigmoid activation function is used to provide the probability of each generator being classified as critical.

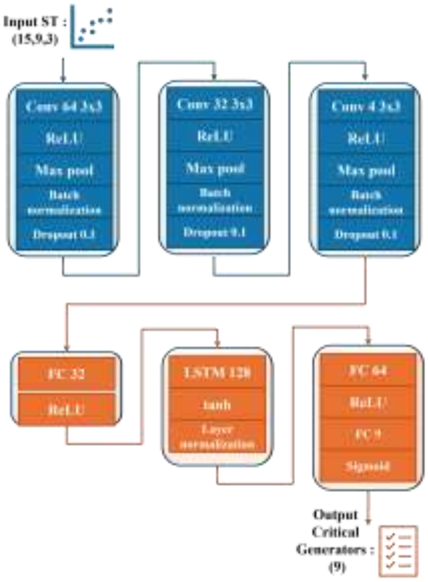

Fig. 8: Model architecture

In addition to the above, training the model requires tuning hyperparameters related to the loss minimization function, the optimization algorithm, the initialization technique, the batch size, and the number of epochs, as well as a β parameter that serves as a regularizer to prevent overfitting during training. Table. 2 summarizes the adjustments made to these hyperparameters.

Table. 2 Model Hyperparameters

Training hiperparameters	Functions / chosen parameters
Loss function	Weighted Cross-Entropy (WCE), β = 0.001
Optimization algorithm	Adam, learning rate = 0.0001
Initialization technic	Gloriot Uniform
Batch size	64
Epochs	1000

4.2.2 Model Training

To train the model, a 140 ms time window is utilized, which corresponds to 15 samples at a sampling PMU frequency of 100 Hz [30]. This window size captures data on the dynamics during the fault and shortly after its clearance from the selected variables (U, θ, δ).

To analyze the training process, the loss function behavior is analyzed (Fig. 9). This function, also known as the cost function, serves as an essential metric for evaluating the performance of machine learning models. The function represents the difference between predictions and actual values, diagnosing issues in learning such as underfitting or overfitting, as well as assessing whether the training and validation sets are adequately representative.

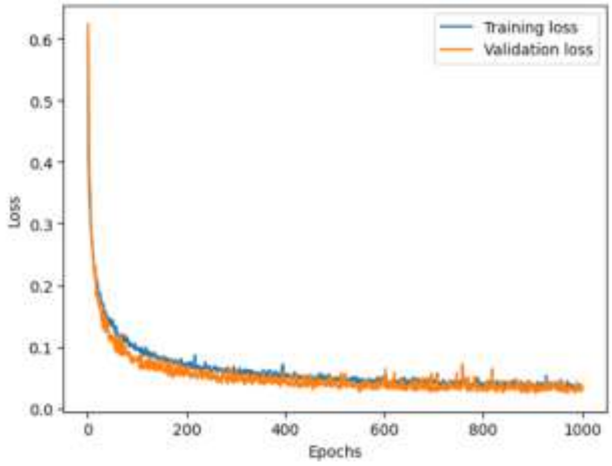

Fig. 9: RCNN Loss function during training

As observed in Fig. 9, after 1,000 epochs, the model has reached a state of convergence. Additionally, there are no signs of overfitting or underfitting between the training and validation function loss, indicating that the model demonstrates a very good potential for generalization.

Furthermore, both algorithms comprising the RCNN model are trained independently to facilitate a comprehensive analysis of their respective training processes. The methods evaluated include a convolutional module (CNN) with three hidden layers containing 64, 32, and 4 filters, respectively, each with a uniform size of 3×3, and an LSTM module with a memory unit of 128 neurons. As illustrated in Fig. 10, the reduction in loss for the hybrid model RCNN converges more quickly compared to the other two models. Although the LSTM-only model achieves a lower final error, it presents a significant degree of overfitting not shown in this work, which limits its generalization capabilities compared to the hybrid model.

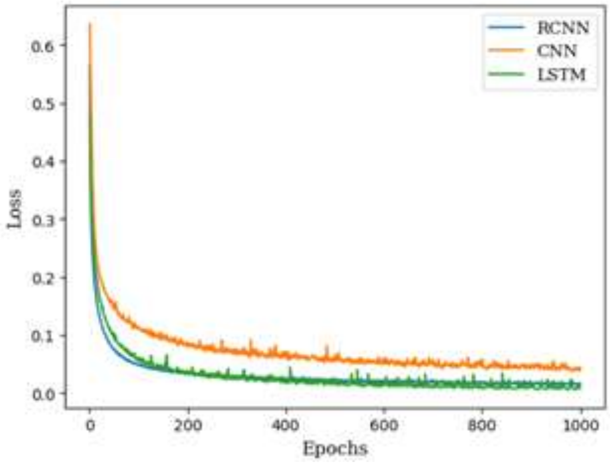

Fig. 10: Comparison of deep learning algorithms

4.3 Performance Results

Following the training process, the RCNN model's performance is evaluated for both the training dataset and the test dataset to verify that it achieves good results with previously unseen cases. In this manner, excellent performance is achieved in the JACC and JACCUE indices, with values exceeding 98%, and a good performance is observed in the JACCUE index, with a percentage greater than 92%. As shown in Table 3, the performance of both datasets is very similar, demonstrating that the model was able to generalize its patterns effectively and achieve favorable results with new data.

Table 3. RCNN Performance Results

Performance metric	Training data	Test data
JACC [%]	99,42	99,3
JACCU [%]	98,02	98
JACCUE [%]	92,77	92,35

To evaluate the effectiveness of the hybrid deep learning model, it has been used the performance results of the two other DL algorithms analyzed (CNN, LSTM). This comparison aims to demonstrate the improvement achieved by combining these two methodologies in the proposed RCNN hybrid model. The performance results of these three models are presented in Table 4.

Table 4. Performance Results for CNN and LSTM Models on test data

Performance metric	CNN	LSTM	RCNN
JACC [%]	99	99,36	99,3
JACCU [%]	96,4	97,38	98
JACCUE [%]	77,64	86,47	92,35

As evidenced in Table 4, the best accuracy results are obtained with the RCNN model. While the CNN and LSTM models achieve good performance for the JACC and JACCU indices. The index that reflects the effectiveness of the task (JACCUE) to be performed is up to 15% lower compared to the model designed in this work. Therefore, the constructed RCNN model not only provides outstanding performance metrics but also proves to be more efficient in its training process compared to other neural network-based models.

4.4 RCNN Real-time Application

The application of the AGTS requires the real-time implementation of the RCNN model. The evaluation delay for the problem depends on the length of the window chosen for the classification tasks of critical generation and the computational capacity of the system on which it is implemented. Given the time necessary for the model implementation and the external delay in real-time operation, Fig. 11 illustrates the total time required for the real-time application of the scheme. This figure illustrates the time window considered for measurement (1), (2), the acquisition of that data by the PMUs, and their transmission (3) as well as the application of the model in real-time (5), accounting for both pre-processing (4) and the signal transfer times for activating the scheme (6) and finally the action of the switches (7).

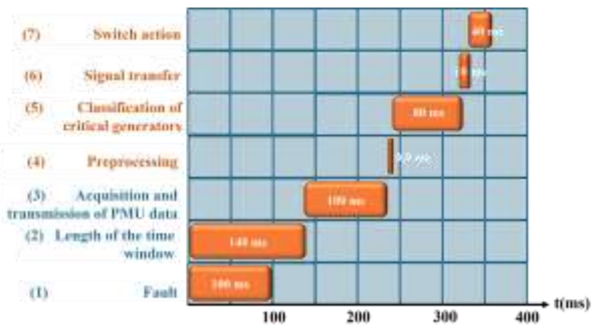

Fig. 11: Timeline of the real-time application of the scheme

In Fig. 12, a real-time event simulation is illustrated, showcasing the time required for the application of the methodology. Although the time needed for model calculations and preprocessing is sufficient to act 300 ms after data acquisition, an additional 100 ms is allowed to account for delays. The control action is performed at 0.5 seconds, considering the calculation times and delays of 400 ms, meaning

400 ms after the start of the dynamic simulation when the failure occurs at 100 ms. Furthermore, the 0.5 seconds also represents the latest moment in the most critical case from the database before reaching 180º. In this sense, the times considered are sufficient to prevent instability in the case that loses transient stability more quickly. The data acquisition times, signal transfer times, and switch action were taken from references, [31], [32].

Additionally, it is possible to observe in Figure 12 the difference in scheme activation at 0.5 seconds in the dynamic response for a generator, as when the control action is taken, the machine remains in synchronism (blue), in contrast to the instability evidenced in orange when this action is not performed.

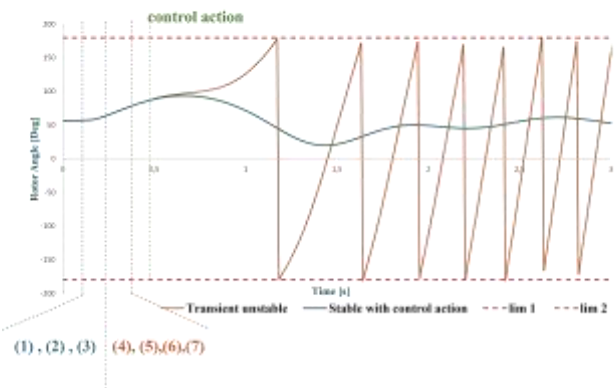

Fig. 12: Real-time case simulation

5 Conclusions

The proposed AGTS was evaluated in a controlled simulation environment using the commonly referenced IEEE New England 39-bus test system Achieving good results. The main conclusions are as follows:

- The methodology presents a promising alternative to traditional generation disconnection schemes, as compared to these, the AGTS considers a vast array of operational scenarios and contingencies. Based on the system's dynamic response to these disturbances, it determines a specific generation disconnection scheme. On the other hand, the methodology involves using a limited number of Phasor Measurement Units (PMUs), needing their deployment only at buses with synchronous generation. In certain countries [33]Regulations require that these generators be equipped with this monitoring technology, making the methodology easily applicable. Additionally, synchronous generators are equipped with automatic tripping, allowing for the methodology to be easily applicable, similar to how a widely used conventional automatic generation disconnection scheme would be implemented.

- This study presents a methodological framework for developing an AGTS that can be applied to any network, given its independence from topology. The primary requirement is to obtain a complete database for model training. It is noteworthy that if the topology changes, the model will need to be retrained. The time required for this retraining can vary depending on computational resources; in the case of the computer used in this research, the training took between 25 and 30 minutes.
- The results of the RCNN model demonstrate high adaptability to operating conditions and the system's response to different contingencies. Additionally, it shows advantages due to the minimal disconnection of plants needed to maintain the system in a stable state.
- The performance metrics results of the RCNN model show high accuracy in avoiding system collapse in more than 92% of cases. Additionally, this model is superior to other deep learning models, such as convolutional networks or LSTM networks separately.
- The analysis of the design and training of the RCNN model demonstrates that it does not exhibit overfitting during the learning process. This indicates that the model performs well with previously unseen cases.
- Considering the times for both calculations, as well as the delays within the system for activating the emergency control scheme, it is shown that the methodology can be used in real-time. An estimated processing time of 300 ms is sufficient to carry out the necessary actions before stability is lost and the system collapses.
- As one of the pillars of this work, the importance of having PMU measurements at generation buses is demonstrated. While some PMUs can estimate the rotor angle, this is not the case for most technologies on the market. In this regard, it is proposed as future work to develop a methodology to estimate this angle based on voltage angle measurements and other measurements typically provided by PMUs.
- Although the methodology was validated using a widely used test system, it does not account for the penetration of non-conventional renewable generation. In this regard, the application of this methodology and the results obtained from a test system with these characteristics would be of great significance, considering current trends.

Acknowledgement:
The authors extend their gratitude to the German Academic Exchange Service (DAAD), which funded the master's study program of Eng. Jorge Enrique Leon Carpio. Without their support, this research work would not have been possible.

Declaration of Generative AI and AI-assisted Technologies in the Writing Process

During the preparation of this work the authors used ChatGPT in order to improve writing and translate paragraphs originally written in Spanish by the author. After using this tool/service, the authors reviewed and edited the content as needed and take full responsibility for the content of the publication.

References:

[1] J. D. E. Echeverria, C. J. C. Cepeda, and D. G. Colome, Real-time transient stability assessment of electric power systems using predictive-SIME based on machine learning, *IEEE PES Innovative Smart Grid Technologies Conference - Latin America (ISGT Latin America)*, IEEE, Quito, Ecuador, Sep. 2017, pp. 1–6. DOI: 10.1109/ISGT-LA.2017.8126760.

[2] M. Pavella, D. Ernst, and D. Ruiz-Vega, *Transient Stability Of Power Systems A Unified Approach to Assessment and Control*, Springer. 2000.

[3] M. Pavella and P. G. Murthy, *Transient stability of power systems: theory and practice*, Wiley. 1994.

[4] Z. S. Al-Shamaain, Hussein. D. Al-Majali, and Bilal. H. Al-Majali, Out-of-Step Detection based on Phasor Measurement Unit, *WSEAS Transactions on Power Systems*, vol. 18, pp. 354–363. Dec. 2023, https://doi.org/10.37394/232016.2023.18.36.

[5] M. A. Obeidat, B. N. Al Ameryeen, A. M. Mansour, H. Al Salem, and A. M. Eial Awwad, Wind Power Forecasting using Artificial Neural Network, *WSEAS Transactions on Power Systems*, vol. 17,

pp. 269–279, Sep. 2022, https://doi.org/10.37394/232016.2022.17.28.

[6] E. Gospodinova, Mathematical Modeling and Planning of Energy Production using a Neural Network, *WSEAS Transactions on Power Systems*, vol. 18, pp. 39–48, Mar. 2023, https://doi.org/10.37394/232016.2023.18.5

[7] G.-V. V. Daniel, Smart Grid Stability Prediction with Machine Learning, *WSEAS Transactions on Power Systems*, vol. 17, pp. 297–305, Jun 2022, https://doi.org/10.37394/232016.2022.17.30.

[8] R. Yousefian and S. Kamalasadan, A Review of Neural Network Based Machine Learning Approaches for Rotor Angle Stability Control, Jan 2017, ArXiv ID: 1701.01214, https://doi.org/10.48550/arXiv.1701.0121.

[9] E. A. Tapia, D. G. Colomé, and J. L. Rueda Torres, Recurrent Convolutional Neural Network-Based Assessment of Power System Transient Stability and Short-Term Voltage Stability, *Energies (Basel)*, vol. 15, no. 23, p. 9240. Dec 2022, DOI: 10.3390/en15239240.

[10] L. Zanella, B. A. S. Ambrósio, G. R. Moraes, I. C. Decker, A. F. C. Aquino, and D. Issicaba, Design of a Machine Learning Model to Enhance the Arming of the System Integrity Protection Scheme of the Brazilian North-Southeast HVDC Bipoles. *Electric Power System Research*, vol 235, p. 110647 Oct 2024, DOI: 10.1016/j.epsr.2024.110647.

[11] Kundur, Prabha & Paserba, John & Ajjarapu, Venkat & Andersson, Göran & Bose, Anjan & Canizares, Claudio & Hill, David & Stankovic, A.M. & Taylor, Carson & Van Cutsem, Thierry & Vittal, V. Definition and Classification of Power System Stability, IEEE/CIGRE Joint Task Force on Stability Terms and Definitions. Power Systems, *IEEE Transactions* on. 19. 1387 – 1401, 2004, DOI: 10.1109/TPWRS.2004.825981.

[12] P. Kundur, *Power System Stability and Control*, McGraw-Hill. 1994.

[13] V. Van Acker, P. Cholley, P. Crossley, C. W. Taylor, and C. Vournas, *System Protection Schemes in Power Networks*, CIGRE, 2001.

[14] S. M. Miraftabzadeh, M. Longo, F. Foiadelli, M. Pasetti, and R. Igual, Advances in the Application of Machine Learning Techniques for Power System Analytics: A Survey, *Energies (Basel)*, vol. 14, no. 16, p. 4776, Aug. 2021, DOI: 10.3390/en14164776.

[15] A. Safavizadeh, M. Kordi, F. Eghtedarnia, R. Torkzadeh, and H. Marzooghi, Framework for real-time short-term stability assessment of power systems using PMU measurements, *IET Generation, Transmission & Distribution*, vol. 13, no. 15, pp. 3433–3442, Aug 2019, DOI: 10.1049/iet-gtd.2018.5579.

[16] S. S. Damodhar and S. Krishna, A Novel Load Shedding Scheme for Voltage Stability, *International Journal of Emerging Electric Power Systems*, vol. 17, no. 6, pp. 649–661, Dec 2016, DOI: 10.1515/ijeeps-2015-0159.

[17] J.-H. Liu and C.-C. Chu, Wide-Area Measurement-Based Voltage Stability Indicators by Modified Coupled Single-Port Models, *IEEE Transactions on Power Systems*, vol. 29, no. 2, pp. 756–764, Mar 2014, DOI: 10.1109/TPWRS.2013.2284475.

[18] J. C. Cepeda, J. L. Rueda, D. G. Colomé, and D. E. Echeverría, Real-time transient stability assessment based on centre-of-inertia estimation from phasor measurement unit records, *IET Generation, Transmission & Distribution*, vol. 8, no. 8, pp. 1363–1376, Aug 2014, DOI: 10.1049/iet-gtd.2013.0616.

[19] L. Wenyuan, *Risk assessment of power systems: models, methods, and applications*. A Jhon Wiley & Sons, 2005.

[20] A. D. Rajapakse, F. Gomez, K. Nanayakkara, P. A. Crossley, and V. V. Terzija, “Rotor Angle Instability Prediction Using Post-Disturbance Voltage Trajectories,” *IEEE Transactions on Power Systems*, vol. 25, no. 2, pp. 947–956, May 2010, DOI: 10.1109/TPWRS.2009.2036265.

[21] R. Zhang, Y. Xu, Z. Y. Dong, and K. P. Wong, “Post-disturbance transient stability assessment of power systems by a self-adaptive intelligent system,” *IET Generation, Transmission & Distribution*, vol. 9, no. 3, pp. 296–305, Feb 2015, DOI: 10.1049/iet-gtd.2014.0264.

[22] T. B. Nguyen and M. A. Pai, "Dynamic security-constrained rescheduling of power systems using trajectory sensitivities," *IEEE Transactions on Power Systems*, vol. 18, no. 2, pp. 848–854, May 2003, DOI: 10.1109/TPWRS.2003.811002.

[23] N. Fei, Y. Gao, Z. Lu, and T. Xiang, Z-Score Normalization, Hubness, and Few-Shot Learning, *IEEE/CVF International Conference on Computer Vision (ICCV),* Montreal, QC, Canada, 2021.

[24] H. Gouk, B. Pfahringer, M. Cree, R. J. Durrant, and K.-E. Kim, Learning Distance Metrics for Multi-Label Classification, *JMLR: Workshop and Conference Proceedings,* Hamilton, New Zealand. Vol 63, pp. 318–333, 2016.

[25] DigSILENT GmbH, "Synchronous Machine," Gomaringen *Germany*, 2018.

[26] DIgSILENT GmbH, "Induction Machine TechRef ElmAsm V2.1," *Gomaringen, Germany*, 2010.

[27] A. Burkov, *The Hundred-Page Machine Learning Book*, vol. 5. Expert Syst., 2019.

[28] S. Ruder, An overview of gradient descent optimization algorithms, 2016, arXiv:1609.04747v2.

[29] K. p. Murphy, *Machine Learning: A Probabilistic Perspective*. MITpress, 2012.

[30] A. von Meier, E. Stewart, A. McEachern, M. Andersen, and L. Mehrmanesh, Precision Micro-Synchrophasors for Distribution Systems: A Summary of Applications, *IEEE Trans Smart Grid*, vol. 8, no. 6, pp. 2926–2936, Nov 2017, DOI: 10.1109/TSG.2017.2720543.

[31] A. ABB, "Live Tank Circuit Breakers-Buyers Guide," 2008, *ABB, Ludvika–Sweden*.

[32] U. Rudez and R. Mihalic, WAMS-Based Underfrequency Load Shedding with Short-Term Frequency Prediction, *IEEE Transactions on Power Delivery*, vol. 31, no. 4, pp. 1912–1920, Nov 2016, DOI: 10.1109/TPWRD.2015.2503734.

[33] ARCONEL, "REGUIACION No. ARCONEL - 003/16," 2016, [Online]. https://vvalner.com/wp-content/uploads/2021/10/SGCR006-409.pdf (Access Date: December 2, 2024).

Contribution of Individual Authors to the Creation of a Scientific Article (Ghostwriting Policy)

- Estefania Tapía, carried out the generation of the database, both operational scenarios and n-1 contingencies.
- Graciela Colomé carried out the supervision, leading the research.
- Jorge León carried out the labelling of the critical generators, the design and training of the deep learning model, the acquisition of results and their corresponding analysis.

Sources of Funding for Research Presented in a Scientific Article or Scientific Article Itself

DAAD Funded master's studies for Engineer Jorge León

Conflict of Interest

The authors have no conflicts of interest to declare.